Hindawi
Shock and Vibration
Volume 2020, Article ID 6414352, 11 pages
https://doi.org/10.1155/2020/6414352

Research Article

Energy Consumption of an Active Vehicle Suspension with an Optimal Controller in the Presence of Sinusoidal Excitations

Jarosław Konieczny, Waldemar Rączka, Marek Sibielak, and Janusz Kowal

AGH University of Science and Technology, Department of Process Control, al. A. Mickiewicza 30, 30-059 Krakow, Poland

Correspondence should be addressed to Jarosław Konieczny; koniejar@agh.edu.pl

Received 25 June 2019; Revised 9 November 2019; Accepted 19 November 2019; Published 12 February 2020

Academic Editor: Luca Landi

Control of vibration is a significant problem in the design and construction of vehicle suspensions. The usage of controlled suspensions is important due to ride comfort, driving safety, and vehicle road holding. The control law for such systems is usually determined as a solution of an optimisation problem with a quality indicator. The effectiveness of vibration reduction is possible to be improved in the entire useful frequency range of a system operation, but usually increasing external energy consumption is observed. An additional problem in the case of vehicle suspensions includes the necessity for increased vibration reduction at selected frequencies. This is related to the natural frequencies of the driver's internal organs or to other reasons. The goal of this work is to find a compromise between efficiency of the suspension in terms of the aforementioned indicators and energy consumption in the presence of sinusoidal excitations. This paper presents a synthesis of a weighted multitone optimal controller (WMOC) for an active vibration reduction system. Energy limitation is taken into account by selection coefficients of the weighting matrix associated with the control signal vector. The control signal in this case is determined on the basis of the parameter estimation of the sinusoidal disturbances vector (PESDV). The vibration transmissibility function and the energetic indicators for the active suspension were determined while taking note of nonlinearities occurring in the actual vehicle. The analysis of energy indicators is presented, depending on the level of vibration reduction efficiency. The results were compared with referencing to LQR control strategy.

1. Introduction

Taking into account the nature of external disturbances caused by road irregularities is an important problem in the design of vehicle suspension structures [1–6]. In general, these disturbances are of a random character [7–10] or of a random character with specified power spectral density (PSD) characteristics depending on the class of the road (ISO 8608) being driven on. From the point of view of the synthesis of the active control system, this spectrum can be broken down into individual enforcing signals with sinusoidal character [11]. Considerations related to the active as well as semiactive reduction of external excitation can be found in many publications [12–20]. The highest vibration reduction efficiency is achieved using the active methods [21–23], but their practical use is limited due to the high energy consumption from the external power source [24–27]. When designing active suspensions [28], it is always necessary to seek a compromise between their effectiveness and energy consumption. This compromise can be achieved by determining the control law as a solution for the optimisation problem [29]. Energy limitation is taken into account when selecting the matrix weighting factors in the adopted quality indicator [21]. By selecting these factors, the efficiency of vibration reduction can be improved in the entire useful frequency range of the system operation. This generally results in an increase in the demand for external energy. In the case of active vehicle suspensions, the necessity for increased vibration reduction at selected frequencies is an additional issue. This applies, for example, to the individual natural frequencies of the driver's and passengers' internal organs or to the need for special vibration reduction for arbitrarily selected frequencies, such as those related to vehicle engine harmonic frequencies or resonant

frequencies of the suspension or other car body parts. The method enabling a solution of this problem is presented in the article [19].

The motivation for presented research was the initial numerical research presented at the IMAC-XXXVI Conference and Exposition on Structural Dynamics in 2018 [30]. This work presents the study of the suspension controlled by a weighted multitone optimal controller (WMOC), with particular emphasis on energy issues. The main goal of the conducted research was improvement of active vehicle suspension efficiency by using the WMOC. The main limitation of active suspensions application is high demand for energy required from the external power source. Limitation of energy consumption, maximal force, and power used by the actuator is the most important challenge put before designers of these suspensions. It is high challenge for those who want to simultaneously assure the high comfort of operator work and sufficient vehicle road holding. Determination of a controller for an active vibration reduction system as a solution of the optimisation task makes it possible to take into account indicators mentioned above.

Because of vibration reduction, the efficiency increase is mainly connected with an increase in energy consumption; therefore, in this paper, optimal control was considered. The objective function takes into account the opposed criteria such as efficiency of vibration reduction and external energy demand. The WMOC satisfies above assumption and additionally allows improving efficiency of vibration reduction for chosen frequencies.

Control synthesis was performed using the WMOC for a parallel active vibration reduction system. A WMOC is determined as a solution of the optimisation problem. Indicators for evaluating the energy properties of active suspensions are suggested. The results of the WMOC tests were compared with the LQR-controlled active suspension test results. In addition to the numerical tests that allow for assessing the suspension comfort, the authors present quality indicators enabling assessment of the demand for external energy necessary to power the active system. The proposed energy indicators for active suspensions are necessary to assess the energy efficiency of the applied controller's operation.

2. Control System with a Weighted Multitone Optimal Controller

2.1. Synthesis Method for a Weighted Multitone Optimal Controller. The weighted multitone optimal controller (WMOC) is determined by solving the optimisation task. The advantage of this approach is the possibility to take note of the energy limitation concerning the controlling signal in the quality indicator. Object condition equations (1) contain a component that takes into account the disturbance being the sum of sinusoidal components $w(t)$ (2). For the correct synthesis of the WMOC controller, it is important to assume that the system with open feedback loop is stable. If this is not the case in the first phase described below, the object-stabilising coupling is implemented.

$$\begin{aligned} \dot{x}(t) &= A_s x(t) + B_u u(t) + B_w w(t), \\ x(0) &= x_0, \end{aligned} \tag{1}$$

$$\begin{aligned} w(t) = \Big(&\alpha_1 \sin\left(\omega_1 t + \varphi_1\right), \ldots, \alpha_j \sin\left(\omega_j t + \varphi_j\right), \ldots, \alpha_{n_w} \\ &\cdot \sin\left(\omega_{n_w} t + \varphi_{n_w}\right)\Big)^T, \end{aligned} \tag{2}$$

where A_s and B are matrices describing the dynamics of the object, A_s is the matrix for which all real parts of the eigenvalues assume negative values, and α_j, ω_j, and φ_j are the amplitude, frequency, and phase of the jth disturbance signal, respectively.

The model of the object described by equations (1) and (2) is nonstationary; it is due to the fact that harmonic disturbances for chosen frequencies ω_j are taken into account. During modelling of the disturbing signal existing in vector $w(t)$, the model of the object could be transformed to its autonomous form which is time-independent. The harmonic disturbances existing in vector $w(t)$ were modelled by equation (3).

$$\begin{aligned} \dot{x}_{d,2j-1}(t) &= \omega_j x_{d,2j}(t), \\ \dot{x}_{d,2j}(t) &= -\omega_j x_{d,2j-1}(t), \\ w_j(t) &= x_{d,2j-1}(t), \\ j &= 1, \ldots, n_w. \end{aligned} \tag{3}$$

Taking into consideration equation (3), the model of the object described by equations (1) and (2) can be rewritten in the autonomous form with extended state vector $\widehat{x}(t)$.

$$\begin{aligned} \dot{x}(t) &= A_s x(t) + B_u u(t) + B_w C_d x_d(t), \\ \dot{x}_d(t) &= A_d x_d(t), \\ x(0) &= x_0, \\ x_d(0) &= x_{d,0}, \\ \widehat{x} &= \left(x^T, x_d^T\right)^T. \end{aligned} \tag{4}$$

On the basis of formula (3), coefficients of matrices $A_d \in R^{2n_w \times 2n_w}$ and $C_d \in R^{n_w \times 2n_w}$ (5) were determined.

$$\begin{aligned} a_{d,l,j} &= \begin{cases} \omega_k, & l = 2k-1, j = 2k, k = 1, \ldots, n_w, \\ -\omega_k, & l = 2k, j = 2k-1, k = 1, \ldots, n_w, \\ 0, & \text{in other cases}, \end{cases} \\ c_{d,l,j} &= \begin{cases} 1, & l = 2k-1, j = 2k-1, k = 1, \ldots, n_w, \\ 0, & \text{in other cases}. \end{cases} \end{aligned} \tag{5}$$

The model of the object described by state equations (4) is time-independent. Amplitudes and phases of disturbing harmonic signal frequencies $w(t)$ are the result of initial conditions $x_{d,0}$ and vector $x_d(t)$. Compound frequencies ω_j of disturbing signal $w(t)$ are the assumed object model parameters. For the considerations presented below, in particular for these frequencies, an improvement of vibration reduction efficiency with minimal energy consumption

is required. To design a controller, a WMOC method was used. The method is described in detail in the literature [31].

In the WMOC synthesis method, a weighted multitone quality indicator is used to evaluate feasible solutions. It allows for the inclusion of energy limitations, independently for each component of the control signal.

During WMOC design, an optimal solution is searched for in a set of control signals $\widetilde{U}$ consisting of continuous and bounded functions for which limits (6) and (7) exist for any ω.

$$u_\alpha = 2 \lim_{T_d \longrightarrow \infty} \frac{1}{T_d} \int_0^{T_d} u(t) \sin(\omega t) \mathrm{d}t, \tag{6}$$

$$u_\beta = 2 \lim_{T_d \longrightarrow \infty} \frac{1}{T_d} \int_0^{T_d} u(t) \cos(\omega t) \mathrm{d}t. \tag{7}$$

In particular, from equations (6) and (7), it results that limits exist for frequency ω_j.

$$u_\alpha^{(j)} = 2 \lim_{T_d \longrightarrow \infty} \frac{1}{T_d} \int_0^{T_d} u(t) \sin\left(\omega_j t\right) \mathrm{d}t, \tag{8}$$

$$u_\beta^{(j)} = 2 \lim_{T_d \longrightarrow \infty} \frac{1}{T_d} \int_0^{T_d} u(t) \cos\left(\omega_j t\right) \mathrm{d}t. \tag{9}$$

Taking into account equations (8) and (9), functions from set $\widetilde{U}$ could be written as formulas (10) and (11):

$$u(t) = \sum_{j=1}^{n_w} u^{(j)}(t) + \breve{u}(t), \tag{10}$$

$$u^{(j)}(t) = u_\alpha^{(j)} \sin\left(\omega_j t\right) + u_\beta^{(j)} \cos\left(\omega_j t\right). \tag{11}$$

This indicator is based on the distribution of control signal $u(t)$ on sinusoidal components $u^{(j)}(t)$, related to the frequency of disturbing signals ω_j.

Taking into account the foregoing, weighted multitone quality indicator [31] is defined using the following equation:

$$J_\omega(x,u) = \limsup_{T_d \longrightarrow \infty} \frac{1}{T_d} \int_0^{T_d} \left(x^T(t) Q x(t) + \sum_{j=1}^{n_w} \left(u^{(j)}(t)\right)^T R_j u^{(j)}(t) \right) \mathrm{d}t. \tag{12}$$

Matrices R_j (positively defined $R_j > 0$) are associated with individual sinusoidal components of the control signal and allow for the inclusion of energy limitations independently for each component. The optimum WMOC is determined by solving the dynamic optimisation task with quality indicator (12) and limitations (1) and (2). The set of control signals $\widetilde{U}$ contains limited continuous functions for which there is a decomposition defined by formulas (8) to (10). Quality indicator J_ω is determined correctly for a set of control signals defined as such. The solution of the optimisation task described by formulas (1), (2), and (12) is determined based on formulas (13) to (16).

$$u_*(t) = \sum_{j=1}^{n_w} u_*^{(j)}(t), \tag{13}$$

$$u_*^{(j)}(t) = \mathrm{Re}\left(K_j\right) w_j(t) + \mathrm{Im}\left(K_j\right) w_{\omega,j}(t), \tag{14}$$

$$K_j = -\left(B_u^T \left(-i\omega_j I_n - A_s^T\right)^{-1} Q \left(i\omega_j I_n - A_s\right)^{-1} B_u + R_j\right)^{-1} \cdot B_u^T \left(-i\omega_j I_n - A_s^T\right)^{-1} Q \left(i\omega_j I_n - A_s\right)^{-1} B_w^{(j)}, \tag{15}$$

$$w_\omega(t) = \left(\alpha_1 \sin\left(\omega_1 t + \varphi_1 + \frac{\pi}{2}\right), \ldots, \alpha_{n_w} \cdot \sin\left(\omega_{n_w} t + \varphi_{n_w} + \frac{\pi}{2}\right)\right)^T, \tag{16}$$

where $B_w^{(j)}$ is the jth column of the B_w matrix, $w_j(t)$ is the jth coordinate of vector $w(t)$, and $i = \sqrt{-1}$.

The solution of the optimisation problem denoted by (1), (2), and (12) is described by (13) to (16). The proof of it is shown in the literature [31].

The solution of the optimisation problem described by formulas (1), (2), and (12) is ambiguous, e.g., by adding any limited signal tending to zero to the optimal control, optimal control is obtained as well. The solution given in formulas (13) to (16) was selected in a manner allowing it to be independent of the initial conditions and of state vector $x(t)$ describing the state of the object without taking into account harmonic disturbances. It is a function of disturbing signals $w(t)$ and the signals offset by $\pi/2$ with respect to the $w(t)$ vector.

Taking into account the model of the object in formulas (4) and (5) independent of time, signal vector $w_\omega(t)$ was formulated in the form

$$w_\omega(t) = C_{d,\omega} x_d(t). \tag{17}$$

Matrix coefficients $C_{d,\omega}$ were determined based on (3).

$$c_{d,\omega,l,j} = \begin{cases} 1, & l = 2k, j = 2k, k = 1, \ldots, n_w, \\ 0, & \text{in other cases.} \end{cases} \tag{18}$$

The WMOC determines optimal control. The control signal is optimal only for sinusoidal components with frequencies $\omega_1, \ldots, \omega_{n_w}$. For other frequencies, the amplitude characteristics of the closed system remain unchanged. For this reason, the synthesis of the controller is divided into two phases.

2.1.1. Phase One. It allows shaping of the frequency characteristics over the entire frequency range. The control signal is determined by solving the classical optimisation problem with the linear quadratic controller (LQR) defined by formulas (19) and (20):

$$J(x,u) = \int_0^\infty \left(x^T(t)Qx(t) + u^T(t)R_0u(t)\right)\mathrm{d}t, \quad (19)$$

$$\begin{aligned} \dot{x}(t) &= Ax(t) + B_u u(t), \\ x(0) &= x_0. \end{aligned} \quad (20)$$

The K_0 controller is determined by solving the Riccati equation:

$$\begin{aligned} PA + A^TP - PB_uR_0^{-1}B_u^TP + Q = 0, \\ K_0 = B_u^TP. \end{aligned} \quad (21)$$

2.1.2. Phase Two. The frequency characteristics are modified for the selected disturbance signal frequencies. The controllers, as mentioned previously, are determined based on the solution of the optimisation task from (1) to (12). Matrix A_s occurring in object state equations (1) is derived from the following formula:

$$A_s = A - B_uK_0. \quad (22)$$

Controllers K_j for each frequency are determined based on formula (15).

The WMOC structure is presented in Figure 1.

2.2. Control System with the WMOC. The WMOC generates a control signal based on the state variables and of course on disturbing signal (14). For calculating $u_*^{(j)}(t)$ of the control signal components, it is required to determine the sinusoidal component vectors $w(t)$ and the $w_\omega(t)$ vector (16) in real time. In the presented control system, these vectors are determined basing on disturbing signal $\xi(t)$. But if disturbance $\xi(t)$ measurement is impossible, the extended state vector $\widehat{x}(t)$ estimator could be used.

In the method which is used in this case, parameters ($w_\alpha^{(j)}$ and $w_\beta^{(j)}$) of signals $w_j(t)$ are estimated on the basis of formulas (23). The time interval equals $[t - T_I^{(j)}, t]$, where $T_I^{(j)}$ is the estimation time and t is the current moment of time.

$$\begin{aligned} w_\alpha^{(j)}(t) &= \frac{1}{T_I^{(j)}} \int_{t-T_I^{(j)}}^{t} \xi(\tau)\sin\left(\omega_j\left(\tau - t + T_I^{(j)}\right)\right)\mathrm{d}\tau, \\ w_\beta^{(j)}(t) &= \frac{1}{T_I^{(j)}} \int_{t-T_I^{(j)}}^{t} \xi(\tau)\cos\left(\omega_j\left(\tau - t + T_I^{(j)}\right)\right)\mathrm{d}\tau, \\ w_j(\tau) &= w_\alpha^{(j)}(t)\sin\left(\omega_j\tau\right) + w_\beta^{(j)}(t)\cos\left(\omega_j\tau\right) \text{ for}, \\ \tau &\in \left[t - T_I^{(j)}, t\right]. \end{aligned} \quad (23)$$

Estimation times $T_I^{(j)}$ can be chosen independently for each jth component. It is good practice to determine it as the multiple of the estimated $w_j(t)$ component period. Signals $w_j(t)$, $w_{\omega,j}(t)$ are determined on the basis of formulas (24) (t is the present moment of time).

$$\begin{aligned} w_j(t) &= w_\alpha^{(j)}(t)\sin\left(\omega_jT_I^{(j)}\right) + w_\beta^{(j)}(t)\cos\left(\omega_jT_I^{(j)}\right), \\ w_{\omega,j}(t) &= w_\alpha^{(j)}(t)\sin\left(\omega_jT_I^{(j)} + \frac{\pi}{2}\right) + w_\beta^{(j)}(t)\cos\left(\omega_jT_I^{(j)} + \frac{\pi}{2}\right). \end{aligned} \quad (24)$$

A short estimation time of components $w_j(t)$, $w_{\omega,j}(t)$ improves the quality of control in the case of variation of disturbance parameters. As a result, estimation times $T_I^{(j)}$ should be assumed as being as short as possible. On the other hand, the shortening of these times aggravates the quality of harmonic component estimation. From the numerical analysis, it is clear that a good compromise is to assume estimation time $T_I^{(j)}$ at the level equal to 10 periods of the estimated sinusoidal component. In the tests carried out later in this study, estimation times $T_I^{(j)}$ were used at the level of 100 periods of the estimated sinusoidal component of the disturbing signal.

Figure 2 shows a diagram of a control system with the WMOC. The K_0 controller closes the feedback loop and is determined in phase one using LQR synthesis. Controllers $K_1, \ldots, K_{n_w}$ are derived from formula (15). Parameter estimation of sinusoidal disturbances vector (PESDV) blocks are used to determine sinusoidal component $w_j(t)$ when ω_j is the frequency of the disturbing signal. These blocks additionally generate signals $\widetilde{x}_{d,2j-1}$ and $\widetilde{x}_{d,2j}$ corresponding to w_j and $w_{\omega,j}$ necessary for the correct operation of controllers K_j. Signals $w_j(t)$, $w_{\omega,j}(t)$ are determined in the PESDV block from formula (24).

3. Synthesis of Active Suspension Based on a WMOC

3.1. Criteria for Assessing the Active Suspension of a Vehicle. The basic criterion for evaluating the suspension system is the vibration transmissibility function. In the case of active suspensions, the energy indicators are important criteria for evaluating suspension work. These criteria were formulated for the quarter suspension of a wheeled vehicle, the scheme of which is shown in Figure 3. The primary function of the suspension system is to reduce the vibrations of mass m_2. The displacement coordinate of sprung mass m_2 is denoted by z_2. The suspension elements were modelled using a parallel connection of spring k_2 and viscous damping b_2. The tyre was modelled using spring k_1 and unsprung mass m_1 (the wheel weight and reduced weight of the suspension arm and suspension components associated with it).

Ideal force-generating element F_s was adopted as the actuator. The disturbance signal from the road is denoted by w. The vibration transmissibility function for the shown suspension in Figure 3 is defined by the following formula:

$$\begin{aligned} T_{z_2,w}(f) &= \frac{z_2^{sk}(f)}{w^{sk}(f)}, \\ z_x^{sk}(f) &= \sqrt{\frac{1}{T_o}\int_0^{T_o}\left(z_x(t) - \overline{z}_x\right)^2\mathrm{d}t}, \\ \overline{z}_x &= \frac{1}{T_o}\int_0^{T_o} z_x(t)\mathrm{d}t, \end{aligned} \quad (25)$$

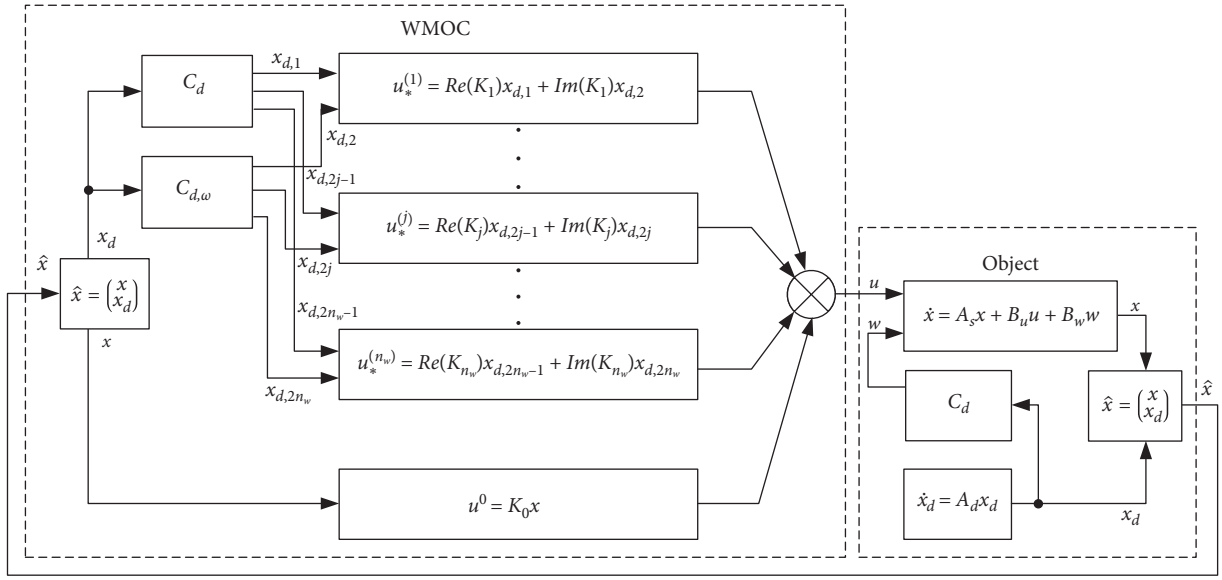

Figure 1: Block diagram of the WMOC.

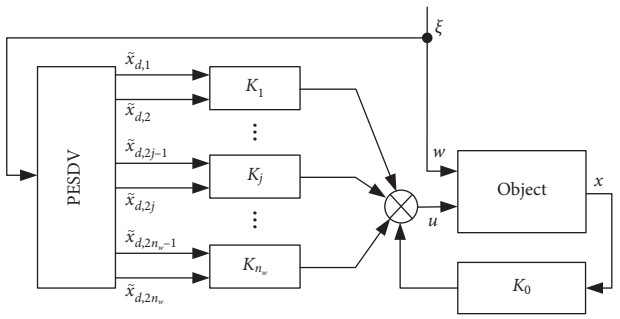

Figure 2: The WMOC control system with the parameter estimation of sinusoidal disturbances.

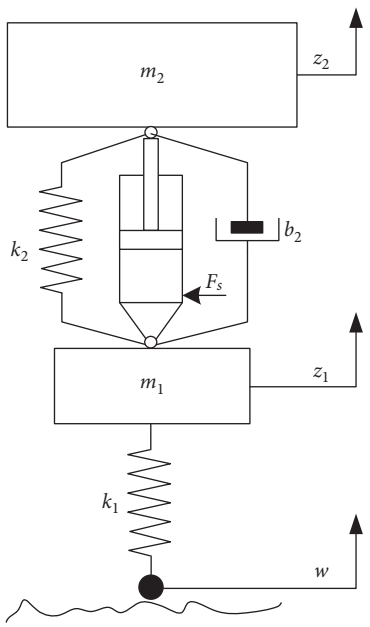

Figure 3: Schematic diagram of the quarter vehicle suspension.

where $z_x \in \{z_2, w\}$.

Active suspension was assessed with regard to energy based on the average energy transferred from or to the power source and instantaneous power analysis on the actuator.

The instantaneous power generated by the actuator is presented by the following formula:

$$P_s(t) = F_s(t)\left(\dot{z}_2(t) - \dot{z}_1(t)\right). \tag{26}$$

One of the basic indicators used in the selection of the actuators is power demand $P_{s,\max}$ (27). This indicator allows for the selection of the power supply unit. The actuators must be selected so that when the control system is operating, the maximum power specified for a given component is not exceeded. Power $P_{s,\max}$ takes positive values. If the $P_{s,\max}$ values for the analysed frequency range were negative, then a controlled energy dissipation element (e.g., based on intelligent materials) should be used as the actuator. Then, the suspension of the vehicle would be a type of semiactive suspensions.

$$P_{s,\max} = \max_t P_s(t). \tag{27}$$

Similarly, for the control system, minimum instantaneous power $P_{s,\min}$ can be defined (28). Power $P_{s,\min}$ may generally assume negative values. This means that in a given control, there is the possibility for energy recovery.

$$P_{s,\min} = \min_t P_s(t). \tag{28}$$

The energy demand of the vibration reduction system can be estimated from the $E_{s,\mathrm{mod}}$ index (29). In this indicator, the modulus of instantaneous power is averaged. Adoption of this definition implies that there is no energy recovery system in the suspension.

$$E_{s,\mathrm{mod}} = \frac{1}{T_o}\int_0^{T_o} \left|P_s(t)\right| \mathrm{d}t. \tag{29}$$

The average energy dissipated in active suspension $E_{s,\text{avg}}$ is determined by formula (30). This energy corresponds to the demand for energy from an external power source in the case of using an ideal energy recovery system.

$$E_{s,\text{avg}} = \frac{1}{T_o}\int_0^{T_o} P_s(t)\mathrm{d}t. \tag{30}$$

The evaluation criteria defined by formulas (27) to (30) were used to compare the energy properties of the WMOC and the reference controller designed using the LQR method.

3.2. Synthesis of a WMOC for Quarter Active Vehicle Suspension. The mathematical model of the active suspension is established from the calculation scheme shown in Figure 3. The equations of force equilibrium are presented by the following formula:

$$\begin{aligned} &m_2\ddot{z}_2 + b_2(\dot{z}_2 - \dot{z}_1) + k_2(z_2 - z_1) = F_s,\\ &m_1\ddot{z}_1 - b_2(\dot{z}_2 - \dot{z}_1) - k_2(z_2 - z_1) + k_1(z_1 - w) = -F_s. \end{aligned} \tag{31}$$

The state vector and input vector are assumed in the following formula:

$$x = (z_2, \dot{z}_2, z_1, \dot{z}_1)^T, \quad u = F_s. \tag{32}$$

Displacement w was assumed as the disturbance signal. Force F_s is the control signal. The state equations are derived from equilibrium force equations (31). State matrix A_s and input matrix B_u needed to determine equation (1) are defined by the following formula:

$$A = \begin{bmatrix} 0 & 1 & 0 & 0\\ -\dfrac{k_2}{m_2} & -\dfrac{b_2}{m_2} & \dfrac{k_2}{m_2} & \dfrac{b_2}{m_2}\\ 0 & 0 & 0 & 1\\ \dfrac{k_2}{m_1} & \dfrac{b_2}{m_1} & -\dfrac{(k_2+k_1)}{m_1} & -\dfrac{b_2}{m_1} \end{bmatrix},$$
$$B_u = \left[0, \frac{1}{m_2}, 0, \frac{-1}{m_1}\right]^T. \tag{33}$$

Matrix B_w is defined by the following formula:

$$\begin{aligned} B_w &= \left[B_w^1, \ldots, B_w^{n_w}\right],\\ B_w^1 &= B_w^2 = \cdots B_w^{n_w} = \left(0, 0, 0, \frac{k_1}{m_1}\right)^T. \end{aligned} \tag{34}$$

All the B_w matrix columns are equal because disturbing signal w is scalar. The following suspension parameters were assumed:

$$\begin{aligned} m_1 &= 35.5\,\text{kg},\\ m_2 &= 365\,\text{kg},\\ k_1 &= 175\,500\,\text{N/m},\\ k_2 &= 20\,000\,\text{N/m},\\ b_2 &= 1\,290\,\text{Ns/m}. \end{aligned} \tag{35}$$

The adopted parameters correspond to the parameters of a light SUV vehicle suspension.

4. Tests of Active Suspension with a WMOC

4.1. Active Suspension with a WMOC. The tests of the WMOC were carried out for the active parallel suspension. The diagram of the quadratic model of this suspension is shown in Figure 3. The parameters taken in the tests correspond to the quarter SUV-type suspension. The reference controller (REF) was designed using the LQR method. It was assumed that the active system guarantees vibration reduction below −10 dB over the entire frequency range, and for arbitrarily selected frequencies (1 Hz, 2 Hz, 3 Hz, 4 Hz, and 5 Hz), the vibration reduction should be greater and be at a level of at least −20 [dB]. These frequencies are selected, for example, from the control band. In a real object, they should be associated with specific frequencies that are relevant to the control goal. The vibration transmissibility functions for the designed controllers (REF and WMOC) are shown in Figure 4.

In the case of REF, the need to provide vibration reduction of −20 dB for some frequencies resulted in a necessity to increase the efficiency of vibration reduction over the entire frequency range to the level of −20 dB or even less.

4.2. Analysis of WMOC Properties. The controllers developed using the LQR method generate the optimum control signal for an object with nonzero initial conditions. In the case of the harmonic disturbing signal, the control signal generated by such a controller is not optimal. On the other hand, the control law in the case of the WMOC is optimal for the harmonic disturbance signals that were assumed during the design phase. In Figure 5, it is shown that for the WMOC at frequencies of 2 Hz, 3 Hz, 4 Hz, and 5 Hz, the force generated by the actuator decreased. At the same time, the vibration reduction for these frequencies is less than −20 dB (Figure 4). This results from the aforementioned fact that in the case of 1 Hz, 2 Hz, 3 Hz, 4 Hz, and 5 Hz frequencies, the WMOC generates an optimal controlling signal.

Figure 5 shows the comparison between the forces generated by the actuator in the case of the WMOC (green line) and REF (red line). The maximum output force generated in the case of the WMOC is 1600 N, whereas in respect of the REF, it is 4250 N. In the frequency range below 2.5 Hz, the forces generated by actuators are similar. In the case of frequencies above 2.5 Hz, the WMOC is characterised by much lower generated force values compared to the reference controller. The use of the WMOC allowed for reducing the requirements concerning the maximum force generated by the actuator—from 4250 N to 1600 N.

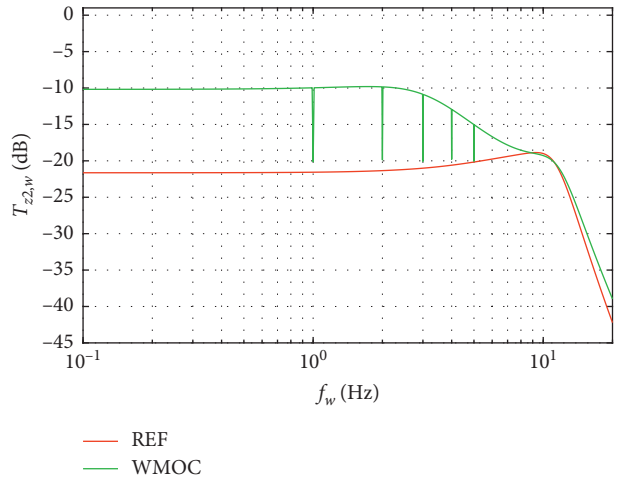

Figure 4: Vibration transmissibility functions for the suspension with the reference controller (REF) and WMOC.

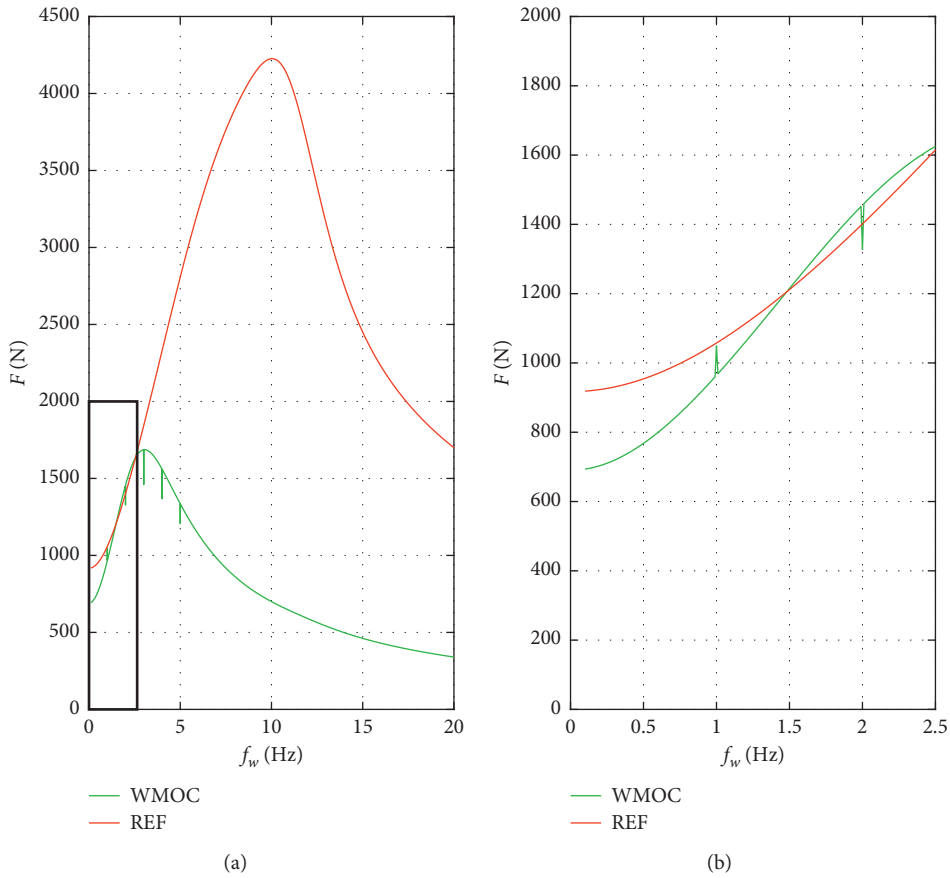

Figure 5: The force generated by the suspension actuator with the WMOC and the reference (REF) controller for 0.05 m induction amplitude.

4.3. Analysis of Energy Properties. As mentioned earlier, one of the basic indicators used in the selection of actuators includes power demand $P_{s,\max}$ (27). Figure 6 shows the comparison between the power demand for an active suspension controlled with the WMOC and the REF reference one. In the case of the WMOC, maximum power $P_{s,\max}$ for the entire frequency range was 2, 831 kW, while for REF, it was 32, 22 kW. Limiting the power requirement from the external power supply allows for limiting its size and price. The $P_{s,\max}$ values are higher for REF over the entire frequency range compared to the values for the WMOC. For the 1 Hz frequency, the $P_{s,\max}$ value for the WMOC and the

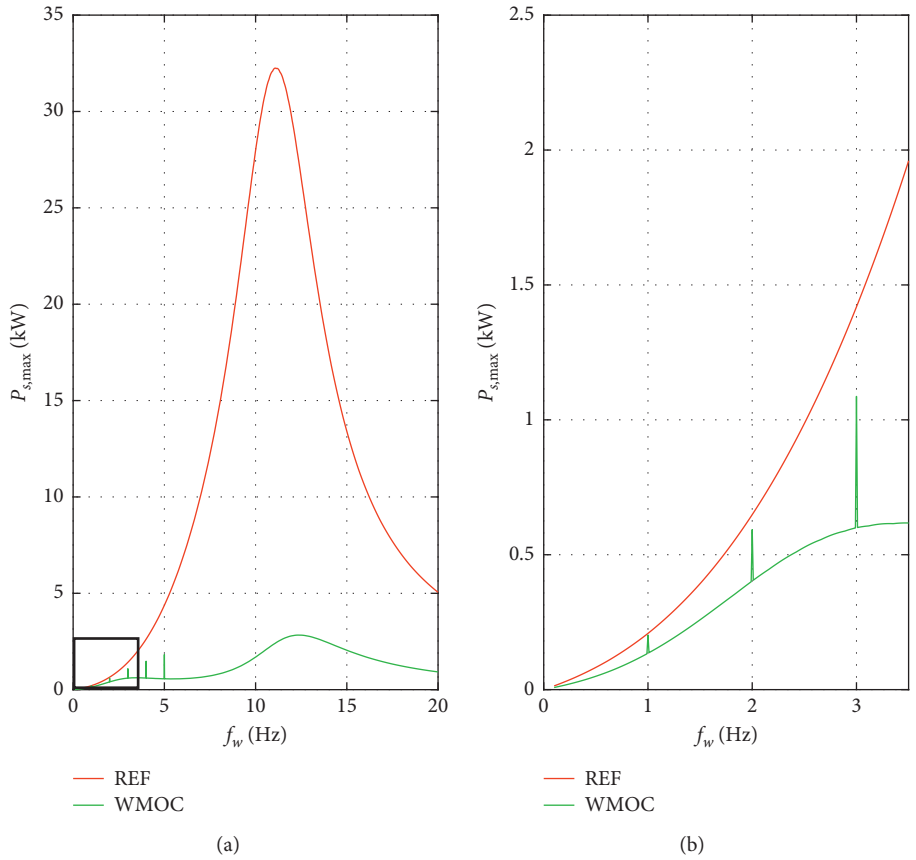

Figure 6: Maximum power generated by the active suspension actuator with the WMOC and the reference one (REF) for 0.05 m induction amplitude.

reference controllers were equal. Above the 3 Hz frequency, the value of $P_{s,\max}$ for the WMOC is much lower than that for the reference controller.

Figure 7 shows minimum power $P_{s,\min}$ (28) emitted at the actuator for the WMOC and the reference one (REF). In the case of both WMOC and REF controllers, power values $P_{s,\min}$ are negative over the entire frequency range. Based on this result, there is a possibility to retrieve energy in both systems.

For frequencies lower than 1.5 Hz, power $P_{s,\min}$ assumes the values which are practically equal, regardless of the controller. In the frequency range between 1.5 Hz and 5.5 Hz, the value of $P_{s,\min}$ is lower for the WMOC, except for the selected frequencies: 1 Hz, 2 Hz, 3 Hz, 4 Hz, and 5 Hz. In the case of the latter frequencies, the $P_{s,\min}$ values are higher for the WMOC than for the reference controller. Based on this result, the possibility to retrieve energy decreases for optimal control of the active suspension. For frequencies ranging from 5.9 Hz to 13.1 Hz, the $P_{s,\min}$ values are much higher for the WMOC. Above the 13.1 Hz frequency, the $P_{s,\min}$ values are similar for both controllers.

The analysis of the WMOC's demand for energy from the external power supply was conducted using criterion $E_{s,\mathrm{mod}}$ defined by formula (29). Figures 8 and 9 show the comparison of the $E_{s,\mathrm{mod}}$ values for the WMOC and the reference controller.

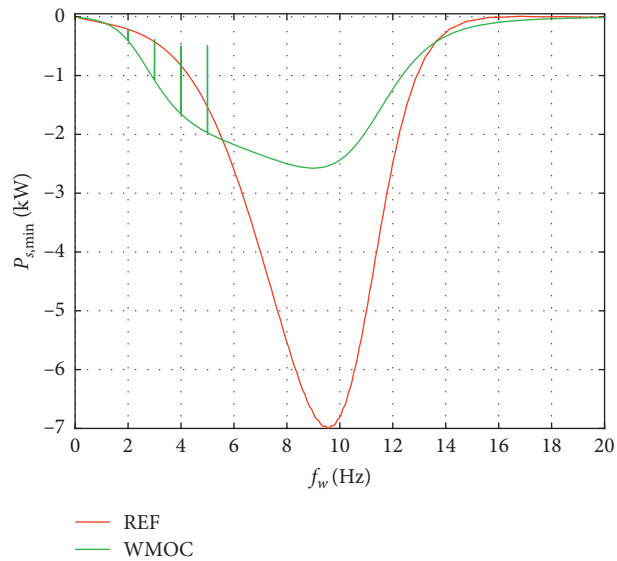

Figure 7: Minimum values of output power at the actuator of the active suspension with the WMOC and the reference controller (REF) for 0.05 m induction amplitude.

Figure 8 shows that over the entire frequency range, the values of $E_{s,\mathrm{mod}}$ are lower for the WMOC than the values achieved by the reference controller. The maximum power

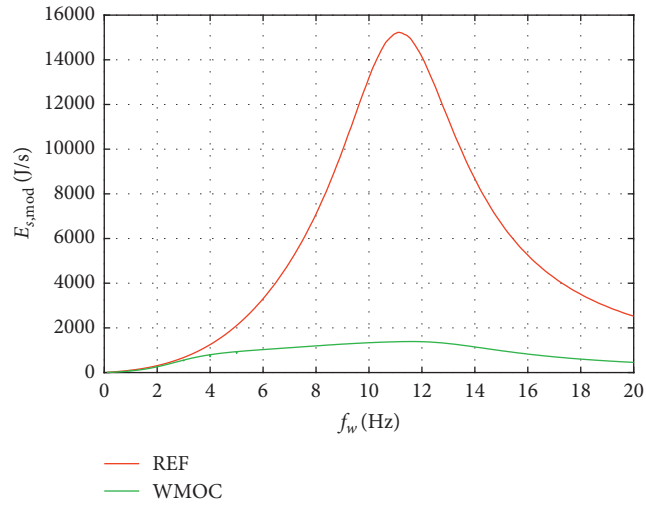

Figure 8: Average energy taken from the external energy source by the actuator with the WMOC and the reference (REF) controllers. Excitation amplitude $A = 0.05$ m.

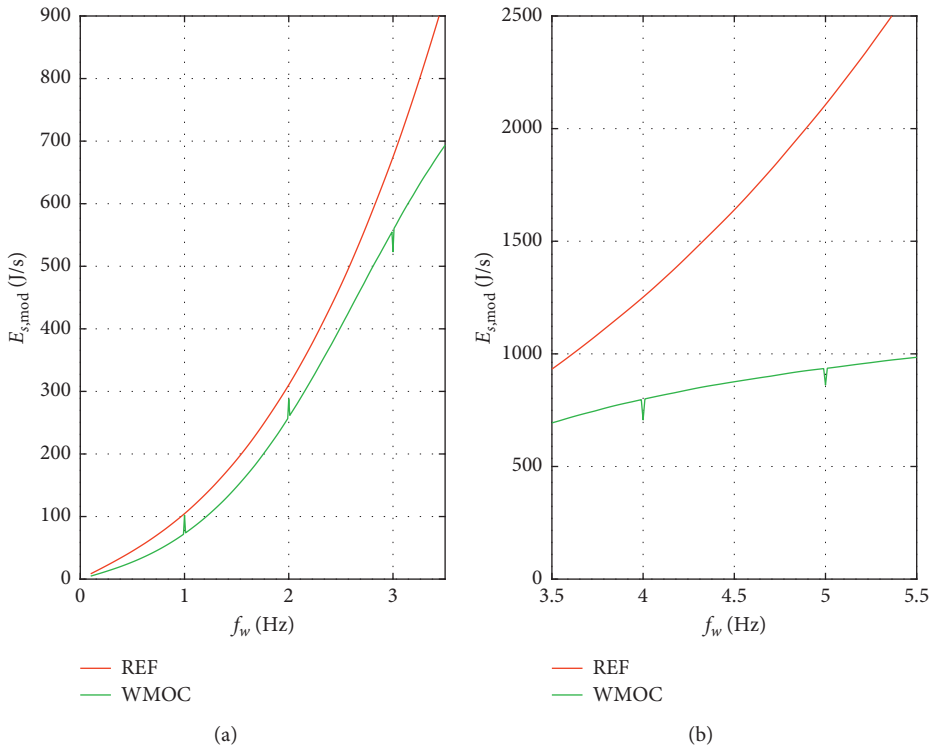

Figure 9: Average energy taken from the external energy source by the actuator with the WMOC and the reference (REF) controllers. The most interesting part (frequency range 0 to 5.5 Hz) of Figure 8 was enlarged.

consumption for the WMOC was 1400 J/s at 11.5 Hz, while for the reference controller, it was 15230 J/s at 11.1 Hz.

Figure 9 shows the graphs of the $E_{s,\mathrm{mod}}$ function in the frequency range up to 5.5 Hz. It can be seen that at 1 Hz and 2 Hz for the WMOC, there was a slight increase in power demand from the external power source. In the case of 3 Hz, 4 Hz, and 5 Hz, the $E_{s,\mathrm{mod}}$ values decreased while obtaining the vibration transmissibility function values below −20 dB.

Figure 10 shows the comparison of average energy $E_{s,\mathrm{avg}}$ (30) taken from the external power source by the WMOC and the REF controllers.

For the WMOC, $E_{s,\mathrm{avg}}$ takes negative values in the frequency range between 1.9 Hz and 10.6 Hz, except for the specific previously chosen frequencies of 3 Hz, 4 Hz, and 5 Hz. Taking this fact into account, the usage of an efficient energy recovery system would allow the reduction of

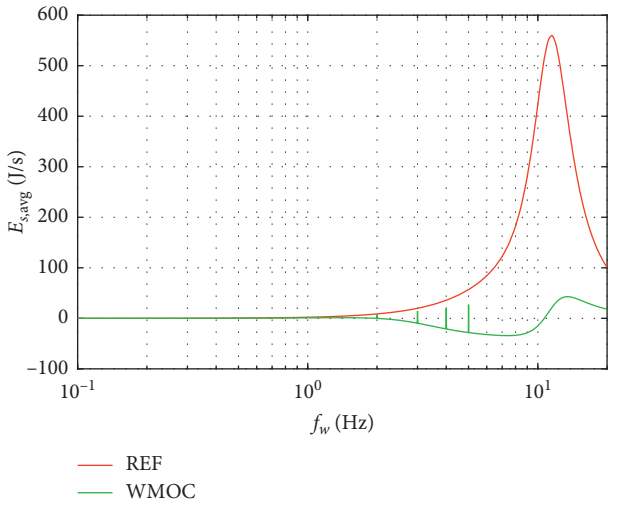

FIGURE 10: Average energy consumed by or returned from the actuator with the WMOC and the reference (REF) controllers. Excitation amplitude $A = 0.05$ m.

vibrations at −10 dB level without an external power supply. The vibration transmissibility function for frequencies of 1 Hz, 2 Hz, 3 Hz, 4 Hz, and 5 Hz is below −20 dB; therefore, $E_{s,\mathrm{avg}}$ values for these specific frequencies are greater than zero.

Estimating the energy consumption in the active suspension would require using the $E_{s,\mathrm{mod}}$ index. Analysis of $E_{s,\mathrm{avg}}$ indicates the possibility of a significant reduction in energy use, if an active suspension is equipped with an energy recovery system.

5. Conclusions

This work presents the study of the energy properties of the WMOC used to control the active suspension of a wheeled vehicle. The results of the study were compared with LQR-controlled suspension studies. It can be seen that the WMOC improves the vibration transmissibility function for selected frequencies while taking into account energy limitation. The control signal generated by the WMOC for these frequencies is optimal, and therefore, it is possible to improve the vibration transmissibility function while limiting the amplitude of the force generated by the actuator. When comparing WMOC and LQR controllers, the use of the WMOC allowed for reducing the requirements concerning the power generated by the actuator when the assumed requirements regarding the vibration transmissibility function were met. Another important parameter is the demand for power of the active vibration reduction system. The WMOC allowed for limiting the power consumption from external power supplies so they could be smaller and cheaper in terms of reduced dimensions and price. The conducted tests demonstrated that the use of the WMOC allows for a significant reduction of the energy requirements in the vibration reduction system. By analysing the criteria for the suspension evaluation, it was found that there was a possibility for improving the energy properties of the active suspension by using an energy recovery system.

Data Availability

The authors declare that all data supporting the findings of this study are available within the article.

Conflicts of Interest

The authors declare that they have no conflicts of interest.

Acknowledgments

This work was supported by the National Centre for Research and Development of Poland (research project no. PBS3/B6/27/2015).

References

[1] C. R. Fuller, S. J. Elliott, and P. A. Nelson, *Active Control of Vibration*, AcademicPress, London, UK, 1996.
[2] C. Hansen and S. Snyder, *Active Control of Noise and Vibration*, E. & F. N. Spon, London, UK, 1st edition, 1997.
[3] D. Karnopp, *Vehicle Stability*, Marcel Dekker, New York, NY, USA, 2004.
[4] A. Preumont and K. Seto, *Active Control of Structures*, Wiley, Hoboken, NJ, USA, 2008.
[5] Z. Lozia and P. Zdanowicz, "Optimization of damping in the passive automotive suspension system with using two quarter-car models," *IOP Conference Series: Materials Science and Engineering*, vol. 148, no. 1, p. 012014, 2016.
[6] Z. Lozia, "A two-dimensional model of the interaction between a pneumatic tire and an even and uneven road surface," *Vehicle System Dynamics*, vol. 17, no. 1, pp. 227–238, 1988.
[7] J. Kasprzyk, P. Krauze, S. Budzan, and J. Rzepecki, "Vibration control in semi-active suspension of the experimental off-road vehicle using information about suspension deflection," *Archives of Control Sciences*, vol. 27, no. 2, pp. 251–261, 2017.
[8] M. Jabłoński and A. Ozga, *Distribution of Random Pulses Acting on a Vibrating System as a Function of its Motion*, Wydawnictwa AGH, Kraków, Poland, 2013.
[9] H. Pang, Y. Chen, J. Chen, and X. Liu, "Design of LQG controller for active suspension without considering road input signals," *Shock and Vibration*, vol. 2017, p. 13, 2017.
[10] H. Pang, Y. Wang, X. Zhang, and Z. Xu, "Robust state-feedback control design for active suspension system with time-varying input delay and wheelbase preview information," *Journal of the Franklin Institute*, vol. 356, no. 4, pp. 1899–1923, 2019.
[11] J. Konieczny, J. Pluta, and A. Podsiadło, "Technical condition diagnosing of the cableway supports' foundations," *Acta Montanistica Slovaca*, vol. 13, no. 1, pp. 158–163, 2008.
[12] M. Jabłoński and A. Ozga, "Determining the distribution of values of stochastic impulses acting on a discrete system in relation to their intensity," *Acta Physica Polonica A*, vol. 121, no. 1A, p. 174, 2012.
[13] C. Maffezzoni, "Hamilton-Jacobi theory for periodic control problems," *Journal of Optimization Theory and Applications*, vol. 14, no. 1, pp. 21–29, 1974.
[14] R. T. Evans, J. L. Speyer, and C. H. Chuang, "Solution of a periodic optimal control problem by asymptotic series," *Journal of Optimization Theory and Applications*, vol. 52, no. 3, pp. 343–364, 1987.
[15] G.-Y. Tang, B.-L. Zhang, Y.-D. Zhao, and S.-M. Zhang, "Optimal sinusoidal disturbances damping for singularly

perturbed systems with time-delay," *Journal of Sound and Vibration*, vol. 300, no. 1-2, pp. 368–378, 2007.

[16] H. Ma, G.-Y. Tang, and W. Hu, "Feedforward and feedback optimal control with memory for offshore platforms under irregular wave forces," *Journal of Sound and Vibration*, vol. 328, no. 4-5, pp. 369–381, 2009.

[17] J. Kwaśniewski, I. Dominik, J. Konieczny, K. Lalik, and A. Sakeb, "Application of self-excited acoustical system for stress changes measurement in sandstone bar," *Journal of Theoretical and Applied Mechanics*, vol. 49, no. 4, pp. 1049–1058, 2011.

[18] J. Konieczny, J. Kowal, W. Raczka, and M. Sibielak, "Bench tests of slow and full active suspensions in terms of energy consumption," *Journal of Low Frequency Noise, Vibration and Active Control*, vol. 32, no. 1-2, pp. 81–98, 2013.

[19] G.-Y. Tang and D.-X. Gao, "Approximation design of optimal controllers for nonlinear systems with sinusoidal disturbances," *Nonlinear Analysis: Theory, Methods & Applications*, vol. 66, no. 2, pp. 403–414, 2007.

[20] R. Bai and D. Guo, "Sliding-mode control of the active suspension system with the dynamics of a hydraulic actuator," *Complexity*, vol. 2018, Article ID 5907208, 6 pages, 2018.

[21] M. Sibielak, J. Konieczny, J. Kowal, W. Raczka, and D. Marszalik, "Optimal control of slow-active vehicle suspension—results of experimental data," *Journal of Low Frequency Noise, Vibration and Active Control*, vol. 32, no. 1, pp. 99–116, 2013.

[22] S. M. Savaresi, C. Poussot-Vassal, C. Spelta, O. Sename, and L. Dugard, *Semi-Active Suspension Control Design for Vehicles*, Elsevier, Amsterdam, Netherlands, 2010.

[23] W. Raczka, J. Konieczny, and M. Sibielak, "Mathematical model of a shape memory alloy spring intended for vibration reduction systems," *Solid State Phenomena*, vol. 177, no. 177, pp. 65–75, 2011.

[24] G. R. Wendel and G. L. Stecklein, "A regenerative active suspension system," in *Vehicle Dynamics and Electronic Controlled Suspensions*, SAE, Warrendale, PA, USA, 1991.

[25] J. Konieczny, "Laboratory tests of active suspension system," *Journal of KONES Powertrain and Transport*, vol. 18, no. 1, pp. 263–271, 2011.

[26] D. A. Crolla, "Theoretical comparisons of various active suspension systems in terms of performance and power requirements," in *Proceedings of the Institution of Mechanical Engineers International Conference on Advanced Suspensions*, London, UK, 1988.

[27] J. Kowal, J. Pluta, J. Konieczny, and A. Kot, "Energy recovering in active vibration isolation system - results of experimental research," *Journal of Vibration and Control*, vol. 14, no. 7, pp. 1075–1088, 2008.

[28] S. Kciuk, S. Duda, A. Mężyk, E. Świtoński, and K. Klarecki, "Tuning the dynamic characteristics of tracked vehicles suspension using controllable fluid dampers," in *Innovative Control Systems for Tracked Vehicle Platforms*, pp. 243–258, Springer, Berlin, Germany, 2014.

[29] S. Wrona and M. Pawelczyk, "Shaping frequency response of a vibrating plate for passive and active control applications by simultaneous optimization of arrangement of additional masses and ribs. Part I: Modeling," *Mechanical Systems and Signal Processing*, vol. 70-71, no. 71, pp. 682–698, 2016.

[30] W. Rączka, M. Sibielak, and J. Konieczny, "Active vehicle suspension with a weighted multitone optimal controller: considerations of energy consumption," in *Proceedings of the Society for Experimental Mechanics*, vol. 6, no. 2, pp. 195–197, Reno, Nevada, 2019.

[31] M. Sibielak, W. Raczka, J. Konieczny, and J. Kowal, "Optimal control based on a modified quadratic performance index for systems disturbed by sinusoidal signals," *Mechanical Systems and Signal Processing*, vol. 64-65, no. 65, pp. 498–519, 2015.